Optical and magnetic properties of porous anodic alumina films embedded with Co nanowires*

Zhang Jing-Jing(张敬晶)[a)b)c)], Li Zi-Yue(李子岳)[a)c)], Zhang Hui-Min(张惠敏)[a)c)], Hou Xue(侯 雪)[a)c)], and Sun Hui-Yuan(孙会元)[a)c)†]

[a)] College of Physics Science & Information Engineering, Hebei Normal University, Shijiazhuang 050024, China
[b)] Department of Medical Physics, Hebei Medical University, Shijiazhuang 050017, China
[c)] Key Laboratory of Advanced Films of Hebei Province, Shijiazhuang 050024, China

(Received 1 April 2013; revised manuscript received 6 May 2013)

A simple method to tune the optical properties of porous anodic alumina (PAA) films embedded with Co nanowires (PAA@Co nanocomposite films) is reported in this paper. The films exhibit vivid structural colors and magnetic properties. The optical properties of the films can be effectively tuned by adjusting the thickness of the PAA template. The deposition of Co nanowires greatly increases the color saturation of the PAA films. The theoretical results of the changes in structural color according to the Bragg–Snell formula are consistent with the experimental results. PAA@Co films can be used in many areas, including decoration, display, and multifunctional anti-counterfeiting applications.

Keywords: nanocomposites, thin films, optical and magnetic properties, porous materials

PACS: 78.66.–w, 42.25.Hz, 61.43.Gt, 75.75.–c **DOI:** 10.1088/1674-1056/22/8/087805

1. Introduction

Structural color in the natural world has attracted the attention of many biologists and physicists.[1,2] It arises mostly from the interference of light in the thin-layer,[3] and multilayers, showing bright colors and luster. In the past few years, a number of artificially colored structures, such as porous silicon and porous aluminum have been investigated for potential applications in sensing and display. Diggle *et al.*[4] reported that a thin PAA film supported on an Al substrate produces a bright color in the visible light range. The colors obtained were bright but the saturation was very low. Wang *et al.*[5] reported that brilliant carbon-coated PAA thin films on an Al substrate were useful for weather-resistant decorative purposes. Afterwards, Xu *et al.*[6] and Sun *et al.*[7] removed the Al substrate of the PPA template and found that the color saturation of the thin alumina film was enhanced to some extent but the films were more fragile.

In order to increase the mechanical strength and expand the range of potential applications of colored PAA films, we fabricate porous anodic alumina films with Co deposited in the pores. Depositing nanowires makes the structural colors more vivid and reduces the fragility. In this paper, we report on the fabrication of such multifunctional films using an alternative current (ac) electrodeposition method. The microstructures of the films are characterized and the optical and magnetic properties are discussed.

2. Experiments

High-purity Al foils (99.999%) were annealed at 673 K for 4 h in an argon atmosphere. The annealed Al foils were electropolished in a mixture of ethanol and perchloric acid (ratio by volume 4:1) for 5 min to smooth the surface. Subsequently, the Al foils were rinsed with acetone and then deionized water and finally dried in air. The Al foils were anodized at a constant direct current voltage of 30 V in 45-g/L phosphoric acid solutions at 292 K for $t_1 = 8$, 8.5, 9, 10, 11.5 min. A graphite plate was used as a counter electrode, and an as-prepared PAA template with aluminum substrate served as the working electrode. The electrolyte contained 0.12-mol/L $CoSO_4 \cdot 7H_2O$ and 0.39-mol/L boric acid. The electrodeposition was carried out at 294 K with an ac voltage of 13 V for 5 min.

In this work, our samples were characterized by a field-emission scanning electron microscope (FE-SEM) and an optical digital camera. Ultraviolet-visible reflectance spectra were measured using a UV-Vis spectrophotometer equipped with an integrating sphere. $BaSO_4$ was used as a reference. The magnetic properties and crystallographic structures of the nanowires were investigated using a physical property measurement system (PPMS) and X-ray diffractometer (XRD), respectively.

3. Results and discussion

Figure 1(a) shows a typical SEM image at the top of a porous anodic alumina (PAA) template. The distribution of

*Project supported by the Natural Science Foundation of Hebei Province, China (Grant No. A2012205038).
†Corresponding author. E-mail: huiyuansun@126.com
© 2013 Chinese Physical Society and IOP Publishing Ltd

the pores is not uniform and the average diameter of the pores is 50 nm. Figure1(b) depicts a typical SEM cross-section image of the PAA@Co nanocomposite film. It can be seen that the column arrays of the film are irregular and the length of the nanowire arrays deposited inside is 160 nm. Figure 2 shows the colors of the PAA@Co nanocomposite films illuminated in natural light, indicating that the colors vary from purple to yellow with increasing anodization time. Because of the deposition of Co nanowires, the color of the reflected light is highly saturated in spite of the highly reflective Al substrate behind the PAA@Co films, as shown in Fig. 3. The detailed explanations will be given as follows.

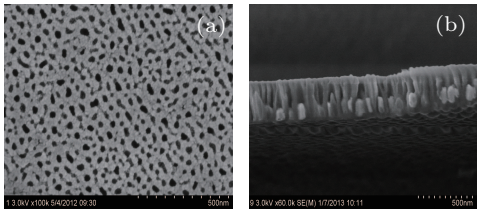


Fig. 1. SEM images of the PAA thin film anodized for 10 min: (a) the top view and (b) the cross-sectional view of the PAA thin film deposited with Co.

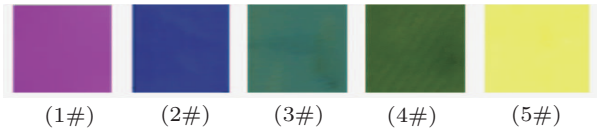


Fig. 2. (color online) The colors of the PAA@Co films with different anodization times: 8 min (1#), 8.5 min (2#), 9 min (3#), 10 min (4#), and 11.5 min (5#).

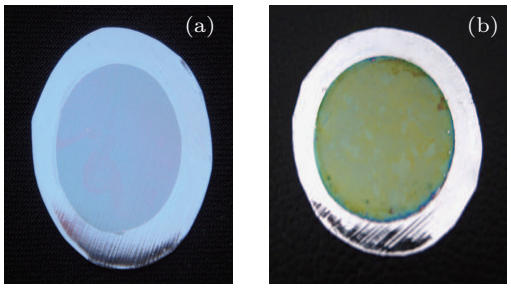


Fig. 3. (color online) Photographs of (a) the PAA anodized for 10 min and (b) the PAA thin film deposited with Co.

The structural colors originate from the constructive interference between the light reflected from the air-AAO interface and the emergent light after reflection on the AAO-Al interference (Fig. 4). This satisfies the Bragg–Snell formula,[8–10]

$$2n_{\mathrm{A}}d_{\mathrm{A}}\cos\theta_{\mathrm{A}}+2n_{\mathrm{B}}d_{\mathrm{B}}\cos\theta_{\mathrm{B}}=\left(m+\frac{1}{2}\right)\lambda. \quad (1)$$

Consider two layers denoted as A (PAA film) and B (PAA@Co film) with thickness values of d_{A} and d_{B}, refraction angles θ_{A} and θ_{B}, respectively, the order of interference m, and the wavelength outside the film λ. The effective refractive indices n_{A} and n_{B} are calculated by the Maxwell–Garnett theory,[11] and are about 1.57 and 1.82, respectively, over the visible wavelength range. As $n_{\mathrm{A}} < n_{\mathrm{B}} > n_{\mathrm{Al}}$, an additional half wavelength should be included in Eq. (1). At $\theta = 0°$, equation (1) can be written as

$$2n_{\mathrm{A}}d_{\mathrm{A}}+2n_{\mathrm{B}}d_{\mathrm{B}}=\left(m+\frac{1}{2}\right)\lambda. \quad (2)$$

The detailed parameters for the film thickness $d_{\mathrm{A}}+d_{\mathrm{B}}$ of the five samples are listed in Table 1, and are measured from the SEM cross-section images. Consequently, the wavelength of the maximum reflectance λ and the order of interference m can be calculated according to the Bragg–Snell formula. The experimental values of λ and m are shown in the reflection spectra (Fig. 5). The results indicate that the experimental values λ in the visible region undergo a red-shift with the increasing film thickness of the samples, which is in accordance with the color changes as shown in Fig. 2. The theoretical values λ from Eq. (2) listed in Table 1 are in good agreement with the experimental results as shown in Fig. 5.

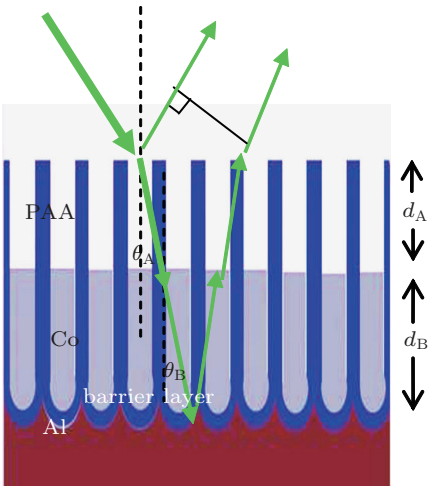


Fig. 4. (color online) The optical processes of a light beam incident on the PAA@Co nanocomposite film.

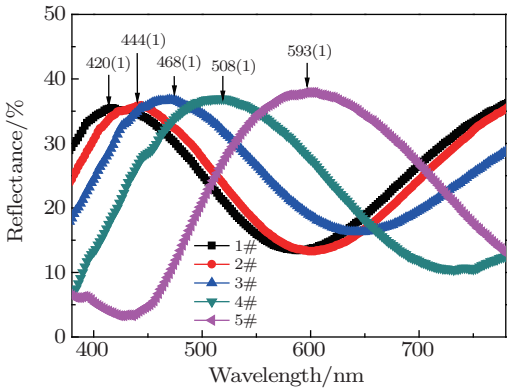


Fig. 5. (color online) The UV-Vis reflection spectra of the nanocomposite films. The wavelength of the maximum reflectance and the corresponding interference order are indicated with vertical arrows.

Table 1. The theoretical values of the order of interference m and the wavelengths of the maximum reflectance λ.

Samples	d_A/nm	d_B/nm	m	λ/nm
1#	24	160	1	438
2#	35	160	1	454
3#	47	160	1	486
4#	70	160	1	534
5#	104	160	1	599

In addition, using an ac electrodeposition method, the Co nanowires are composed of loose grains, which absorb part of the incident and reflected light from the AAO–Al interface, leading to the enhancement of the color saturation. According to the difference in color saturation before and after deposition, some patterns can be recorded on PAA thin films as shown in Fig. 6. Here, the procedure for fabricating the pattern was as follows. First, the desired pattern was painted with colorless ink on the top surface of the PAA template. Then, Co was deposited in the pores of the PAA template. Finally, the ink was removed with acetone leaving the patterns.

Figure 7 shows the XRD patterns of the Co nanowires in the PAA template. They show that Co presents an hcp phase and Co (101) is the preferred orientation.

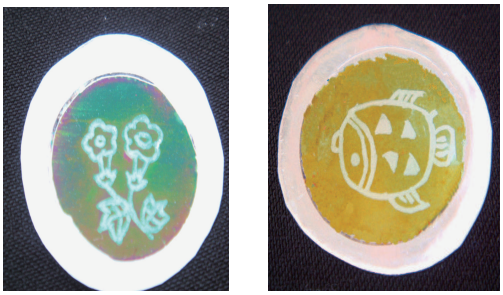


Fig. 6. (color online) Photographs of the patterned PAA@Co nanocomposite films.

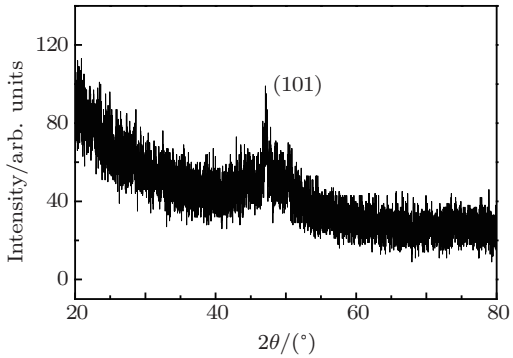


Fig. 7. The XRD diffraction pattern of the PAA@Co nanocomposite film.

The magnetic properties of the nanocomposite films with different anodization times are measured using a PPMS at room temperature. Hysteresis loops of the Co nanowires synthesized in the PAA template with the applied field parallel to the wires are shown in Fig. 8. It can be seen that the hysteresis loops almost overlap, suggesting that the magnetic signals change little as the color varies. This is attributable to the fact that the same deposition times for the Co nanowires were used in all cases. The M–H curves obtained with the field applied in the directions parallel ($H_{\parallel}$) and perpendicular ($H_{\perp}$) to the Co nanowires are alike, as shown in the inset of Fig. 8, indicating that the Co nanowires show no apparent magnetic anisotropy. This can be understood as follows. Shape anisotropy favors the alignment of the magnetization along the long axis of the wire. The XRD results show that Co (101) is the preferred orientation rather than the c axis (the long axis of the wire), suggesting that magnetocrystalline deviates from the long axis of the wires. Under the combined effect above, the orientations of the magnetic moments present a fan-shaped distribution and the Co nanowires show no magnetic anisotropy.

In addition, we can calculate the value of coercivity by adopting the fanning reversal mode. According to the size of the magnetic grain, each nanowire consists of three magnetic grains that are randomly distributed in the template. For our sample, the magnetization intensity is 565 emu/cm^3. The coercivity parallel to the wire is calculated to be 465 Oe (1 Oe = 79.5775 A·m^{-1}), which is in good agreement with the previous experimental value of 475 Oe, suggesting that the coercivity mechanism of the Co nanowires is indeed described by the fanning mode.

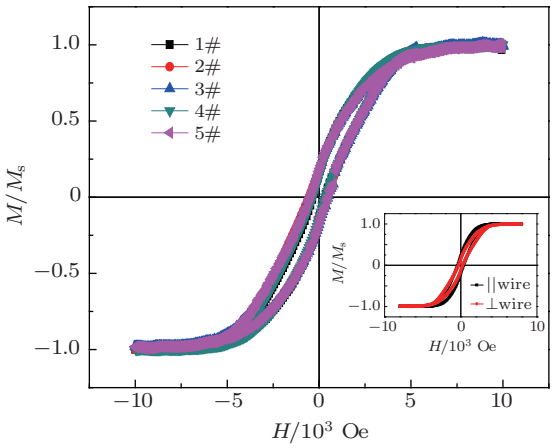


Fig. 8. (color online) Hysteresis loops of the PAA@Co nanocomposite films with the applied field perpendicular to the wires. The inset shows the hysteresis loops of a PAA@Co composite film with the applied field parallel and perpendicular to the Co nanowires.

4. Conclusions

PAA@Co functional nanocomposite films with structural color and magnetic properties are synthesized by an ac electrodeposition method. Theoretical analyses on the wavelength of maximum reflectance and the order of interference according to the Bragg–Snell formula are in good agreement with the

results measured by the UV-Vis spectrophotometer. Hysteresis loops show that the magnetic signals of the Co embedded in the nanocomposite films remain constant with changing color. The magnetization reversal mechanism is in accordance with the fanning reversal mode. Such colorful films can be used in multifunctional anti-counterfeit technology.

References

[1] Xu Q, Yang Y H, Liu L H, Gu J J, Liu J J, Li Z Y and Sun H Y 2012 *J. Electrochem. Soc.* **159(1)** C25

[2] Sheng C C, Cai Y Y, Dai E M and Liang C H 2012 *Chin. Phys. B* **21** 088101

[3] You H L and Zhang C F 2009 *Chin. Phys. B* **18** 349

[4] Diggle J W, Downie T C and Goulding C W 1969 *Chem. Rev.* **69** 365

[5] Wang X H, Akahane T, Orikasa H, Kyotani T and Fu Y Y 2007 *Appl. Phys. Lett.* **91** 011908

[6] Xu Q, Yang Y H, Gu J J, Li Z Y and Sun H Y 2012 *Mater. Lett.* **74** 137

[7] Sun H Y, Zhang H M, Hou X, Liu L H, Wu T S and Yang S M 2013 *J. Mater. Chem. C* **1** 3569

[8] Míguez H, Blanco A, Meseguer F, López C, Yates H M, Pemble M E, Fornés V and Mifsud A 1999 *Phys. Rev. B* **59** 1563

[9] Liu Y S, Chang Y, Ling Z Y, Hu X and Li Y 2011 *Electrochem. Commun.* **13** 1336

[10] Kinoshita S and Yoshioka S 2005 *Chem. Phys. Chem.* **6** 1442

[11] Maxwell Garnett J C 1906 *Philos. Trans. R. Soc.* **205** 237

[12] Jacobs I S and Bean C P 1955 *Phys. Rev.* **100** 1060